PROGRESS IN PHOTOVOLTAICS: RESEARCH AND APPLICATIONS
Prog. Photovolt: Res. Appl. 2008; **16**:609–613
Published online 10 July 2008 in Wiley InterScience (www.interscience.wiley.com) DOI: 10.1002/pip.839

Applications

The Implementation of Temperature Control to an Inductive-Coil Photoconductance Instrument for the Range of 0–230°C

B. B. Paudyal[1*,†], K. R. McIntosh[1], D. H. Macdonald[1], B. S. Richards[2] and R. A. Sinton[3]
[1]*College of Engineering and Computer Science, The Australian National University, Canberra, ACT 0200, Australia*
[2]*School of Engineering and Physical Sciences, Heriot-Watt University, Edinburgh EH14 4AS, Scotland, UK*
[3]*Sinton Consulting Inc., 1132 Green Circle, Boulder, CO 80305, USA*

A new device setup for temperature and injection-dependent lifetime spectroscopy (TIDLS) is described. It comprises two off-the-shelf components: a heating and cooling stage (HCS) from INSTEC and an inductive-coil photoconductance (PC) instrument (WCT-100) from Sinton Consulting Inc. The HCS was fitted to the WCT-100 in a manner that circumscribes the inductive coil (the sensor) of the RF bridge circuit and controls the temperature of the wafer effectively. This setup has the advantage of requiring minor modifications to industry standard instruments while attaining a large temperature range. As experimental verification, injection-dependent lifetimes were measured over a temperature range, 0–230°C, in three iron-implanted silicon wafers. The measured lifetimes are consistent with the Shockley–Read–Hall equation using the impurity concentration calculated from the implant dose and the energy level and capture cross-sections of interstitial iron from the literature. Copyright © 2008 John Wiley & Sons, Ltd.

KEY WORDS: TIDLS; lifetime; photoconductance; contactless

Received 30 October 2007; Revised 1 May 2008

INTRODUCTION

The inductive-coil photoconductance (PC) lifetime measurement is one of the most popular characterisation techniques in the photovoltaic industry. It has the advantages of being contactless and capable of measuring lifetimes over a wide range of injection levels in a few seconds. Temperature and injection-dependent lifetime spectroscopy (TIDLS) is a defect characterisation technique based on such lifetime measurement and is considered to provide relatively unambiguous characterisation of defect parameters in comparison to injection-dependent lifetime spectroscopy alone.[1]

The first TIDLS instrument was developed and tested on an aluminium-doped silicon sample by Schmidt *et al*.[2] They analysed their data to determine the defect energy E_t and temperature dependence of the capture cross-section ratio σ_n/σ_p. The measurement device consisted of an inductive-coil PC instrument (WCT-100) from Sinton Consulting Inc.[3] with a brass ring capable of heating the sample from 30°C to 150°C. A similar setup was used by Diez *et al*.[4,5] and Brikholz *et al*.[6] for the measurement of E_t, σ_n/σ_p

* Correspondence to: B. B. Paudyal, College of Engineering and Computer Science, The Australian National University, Canberra, ACT 0200, Australia.
† E-mail: bijaya.paudyal@anu.edu.au

and the trap density N_t of tungsten- and cobalt-contaminated silicon, and the measurement of E_t, σ_n and σ_p, of iron-contaminated boron-doped silicon samples. TIDLS analyses have been performed over a wider temperature range by Roth *et al.*[7] using a photoluminescence (PL) detector to measure E_t of titanium-contaminated boron-doped silicon, and by Rein *et al.*[8] using a microwave PC detector to determine E_t and σ_n/σ_p of molybdenum-contaminated silicon. Rein *et al.*[9] have also combined the temperature-controlled microwave detector and inductive-coil PC instruments to characterise recombination in iron-contaminated boron-doped silicon.

The purpose of this work was to develop a relatively simple means to apply TIDLS over a large temperature range. Like earlier researchers,[3–5] the TIDLS apparatus consisted of a WCT-100 PC instrument combined with a temperature controller. But rather than the brass ring configuration, which provided a relatively unstable method to control the sample temperature over the range, 30–150°C, this system incorporates a modified INSTEC temperature controller, which is in principle capable of controlling the sample temperature from −190 to 400°C. In this work, the proof of concept is demonstrated with iron-contaminated silicon wafers over the range of 0–230°C.

The decision to use an inductive-coil PC based system was manifold. Firstly, the WCT-100 is widely distributed in the photovoltaic industry, being used by more than 200 research institutions,[3] making it a well-understood instrument and a good base to construct the apparatus. Secondly, unlike microwave PC instruments, inductive-coil PC does not require a bias light that needs to be adjusted for each data point, and enables an absolute measurement of lifetime rather than a differential measurement. Thirdly, inductive-coil PC is suitable for measurements over a very wide injection range, unlike microwave PC and PL.[7] While PC measurements have the disadvantage of being affected by trapping, as observed in multi-crystalline silicon,[10] and by depletion-region modulation, as occurs for samples with a *p–n* junction,[11] these complications are usually avoided by examining mono-crystalline silicon without *p–n* junctions.

EXPERIMENTAL SETUP

The WCT-100 from Sinton Consulting Inc.[3] was combined with a heating and cooling stage (HCS) supplied by INSTEC,[12] as shown in Figure 1. Both

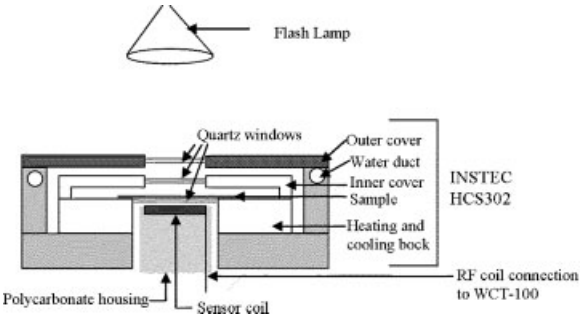

Figure 1. Experimental setup of PCD-based TIDLS system

instruments required modification. In the case of HCS, the HCS302 model was modified by INSTEC to house samples of up to $5 \times 5\,cm^2$. Its upper apertures were increased to 2·0 cm diameter to permit a larger illumination area, and the rear aperture was increased to 2·2 cm diameter to permit the insertion of an inductive coil close to the sample. In the case of the WCT-100, the diameter of the inductive coil was reduced to 1·0 cm and encapsulated by a polycarbonate cylinder for structural stability. The cylinder was inserted into the rear aperture of the HCS302 such that the coil was ∼2 mm from the sample, separated by an air gap and a quartz window as shown in Figure 1.

The inner (sample) chamber of the HCS302 is either heated with resistive elements using switching PID control or cooled by circulating liquid nitrogen inside the same system. The external components of the HCS302 are kept close to the room temperature by circulating water through ducts within the outer chamber.

CALIBRATION

A calibration of the bridge circuit over the temperature range, 0–230°C, was performed using three wafers of known boron-dopant concentration. Their conductance was calculated using the carrier mobility model of Raggioni *et al.*[13] This model was selected because of its operability over a large temperature range and low error in comparison to those of Arora *et al.*[14] and Dorkel *et al.*[15] Figure 2 plots the output voltage under dark conditions V_{out} against the sheet conductance of the reference wafers for temperatures ranging from 0 to 230°C. A least-squares linear fit to the data at each temperature yielded a slope within the range

DOI: 10.1002/pip

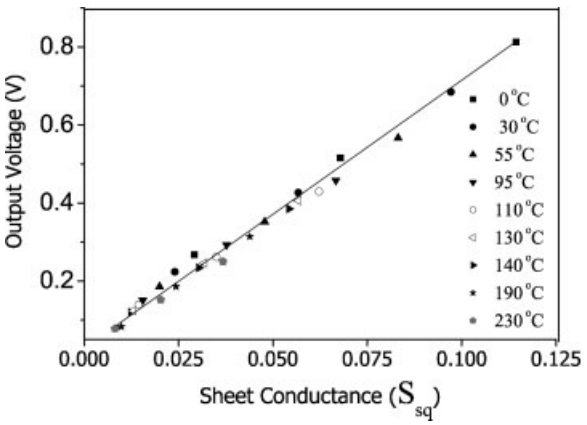

Figure 2. Calibration of the system for the sample temperature range, 0–230°C, under dark conditions

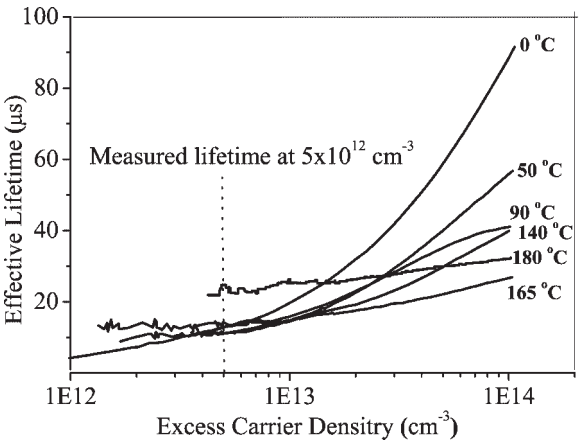

Figure 3. Lifetime curves of Fe-contaminated sample measured over a range of temperature for 100 Ω cm wafer

$6{\cdot}46 \pm 0{\cdot}28$ S/V, with no obvious trend between slope and temperature. We used this value and uncertainty to calibrate the system in the experiment described below. Incidentally, a single least-squares linear fit to all data yields a slope of $6{\cdot}67 \pm 0{\cdot}06$ S/V, where the uncertainty represents the 95% confidence limit.

The calibration process was time consuming because the LC circuit was balanced for every temperature and wafer. In future, the calibration time will be reduced significantly by the application of a technique that utilises a single wafer whose resistivity is adjusted by steady-state illumination.[16]

The temperature of the wafer was also calibrated to the temperature of the HCS stage. The temperature variation within the wafer was at most 5°C, as measured by thermocouples attached to a representative test wafer. The samples were always placed in the same position in relation to the temperature stage and inductive coil to minimise error.

EXPERIMENTAL VERIFICATION

The accuracy of the instrument was tested using three boron-doped silicon samples that had been intentionally contaminated with iron. Each sample was implanted with an iron dose of $1 \times 10^{11}\,\mathrm{cm}^{-2} \pm 20\%$, $\pm 20\%$, annealed at 900°C for 1 h to distribute the iron within the sample, and coated with PECVD silicon nitride to ensure that surface recombination was negligible relative to the bulk recombination. The samples differed by their resistivity: 100, 13 and 1.0 Ω cm.

PC lifetime measurements were taken before and after light soaking at temperatures ranging from 0 to 230°C. The interval between measurements was more than 20 min, which is sufficiently greater than the dissociation time constant of Fe/B pairs 13–18 s to ensure the samples were in steady-state.[17] Figure 3 plots the pre-soaking effective carrier lifetime τ_{eff} of the 100 Ω cm wafer as a function of excess carrier density Δn and temperature, providing an example of the system's output. Figures 4–6 plot τ_{eff} at a particular Δn (listed in the figure) as a function of temperature in an Arrhenius plot. In each case, the squares plot τ_{eff} before light soaking and the circles plot τ_{eff} after light soaking. (Unfortunately, the 100 Ω cm sample broke prior to light soaking, and only one set of data was obtained.) Note that at the chosen Δn, all samples were in low-level injection, which simplifies the analysis.[1] The error bars were determined from a combination of the uncertainty in the temperature (3%), the wafer thickness (2%) and therefore mentioned calibration (4%).

The data of Figures 4–6 show that the pre-light soaking τ_{eff} deviates from the post-light soaking τ_{eff} below some temperature that depends on the boron concentration. The lifetime is higher prior to light soaking because the interstitial iron (Fe_i) forms Fe/B pairs, which have a lower recombination rate than the Fe_i defects.[6,9] These results are consistent with Reference.[9] exhibiting the same trend and comparable

DOI: 10.1002/pip

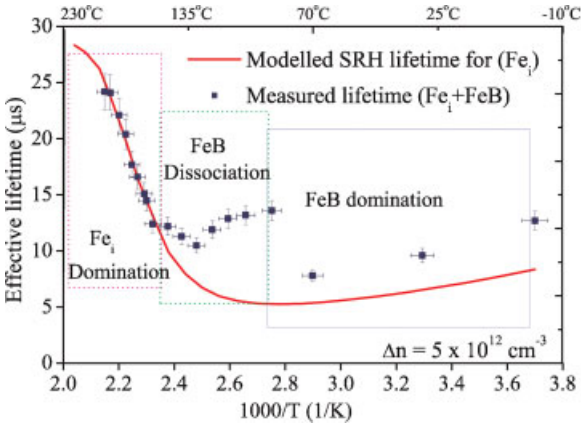

Figure 4. Arrhenius plot of lifetime SRH model and measured data for 100 Ω cm wafer

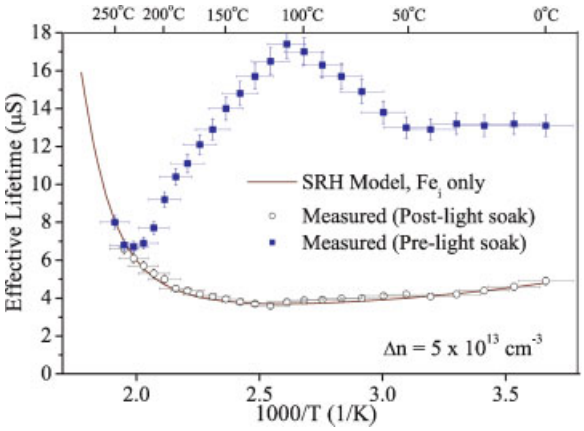

Figure 6. Arrhenius plot of effective lifetime SRH model and measured data for 1 Ω cm wafer

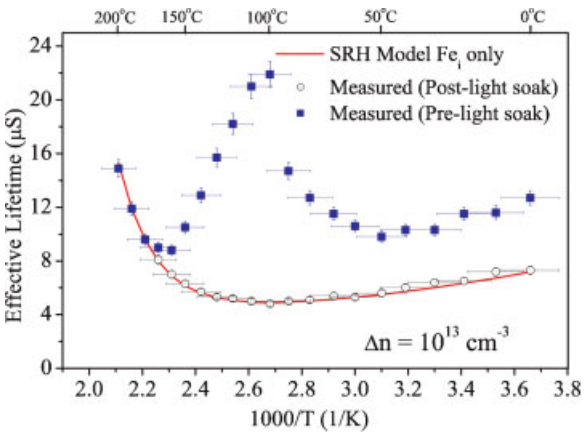

Figure 5. Arrhenius plot of lifetime SRH model and measured data for 13 Ω cm wafer

magnitudes. This pre-light soaking data have been included as a matter of interest, but the real verification of the apparatus comes from the post-light soaking data.

After light soaking, Fe/B pairs disassociate leaving Fe_i as the dominant defect.[6,9] The resultant trend between τ_{eff} and temperature is consistent with the theoretical SRH equation, plotted as a line in each figure. Three of the recombination parameters in the SRH equation were taken from the literature: $E_t - E_v = 0{\cdot}394$ eV,[1] $\sigma_n(Fe_i) = 10^{-10} \times T^{-1{\cdot}5}$ cm^2 [18] and $\sigma_p(Fe_i) = 2{\cdot}8 \times 10^{-16} \times \exp(-0{\cdot}043/kT)$ cm^2,[18] N_t was adjusted to attain a best fit to the post-light soaking data. (In the case of the 100 Ω cm wafer, N_t was determined by fitting the pre-light soaking data at temperatures greater than 155°C for which the contribution from the Fe/B defect is negligible.[9,19] Table I presents the results, showing that the best-fit value of N_t agrees well with N_t determined from the dose and the cross-over point at room temperature.[20,21]

The results of these experiments support the accuracy of the system. While this temperature-dependent analysis of τ_{eff} has been conducted at a single carrier concentration, the system is, of course, also compatible with injection-dependent analyses.

Table I. Wafer resistivity, Fe dose, width, N_t determined from the cross-over point (COP) method at room temperature, and N_t that provides the best fit to the data of Figures 4–6

Resistivity (Ω cm)	Dopant conc. (cm^{-3})	Fe dose (cm^{-2})	Width (μm)	N_t from dose/width (cm^{-3})	N_t from COP (cm^{-3})	Best fit N_t (cm^{-3})
100	$1{\cdot}2 \times 10^{14}$	1×10^{11}	216	$4{\cdot}6 \times 10^{12}$	11×10^{12}	$9{\cdot}2 \times 10^{12}$
13	$1{\cdot}0 \times 10^{15}$	1×10^{11}	445	$2{\cdot}2 \times 10^{12}$	$5{\cdot}2 \times 10^{12}$	$2{\cdot}2 \times 10^{12}$
1·0	$1{\cdot}2 \times 10^{16}$	1×10^{11}	490	$2{\cdot}0 \times 10^{12}$	$3{\cdot}0 \times 10^{12}$	$1{\cdot}7 \times 10^{12}$

DOI: 10.1002/pip

CONCLUSION

A TIDLS system has been constructed from an HCS from INSTEC and a PC lifetime instrument from Sinton Consulting Inc. The system's calibration was described and found to be linear over the range 0–230°C. The accuracy of the system was supported by lifetime measurements on three iron-contaminated boron-doped silicon wafers, where the results were consistent with the SRH equation using recombination parameters from the literature and the iron implantation dose. The described TIDLS system provides a useful and relatively inexpensive way to measure a wafer's lifetime over a wide range of well-controlled temperatures.

Acknowledgements

The authors thank Henry Zou from Instec Inc. (CO, USA) and Bruce Condon from CECS, ANU for their technical help, and Pietro Altermatt from University of Hannover for his assistance with the carrier mobility models. This work was funded by an Australian Research Council Linkage Grant between the Australian National University, SierraTherm Production Furnaces and SunPower Corporation.

REFERENCES

1. Rein S. *Lifetime Spectroscopy—A Method of Defect Characterization in Silicon for Photovoltaic Applications*. Springer: Berlin, 2005.
2. Schmidt J. Temperature and injection dependent lifetime spectroscopy for the characterization of defect centers in semiconductors. *Applied Physics Letters* 2003; **82**: 2178–2180.
3. www.sintonconsulting.com, 08 August 2007.
4. Diez S, Rein S, Glunz SW. Analyzing defects in silicon by temperature and injection dependent lifetime spectroscopy (T-IDLS). *20th European PVSEC*, Barcelona, 2005.
5. Diez S, Rein S, Roth T, Glunz SW. Cobalt related defect levels in silicon analyzed by temperature and injection dependent lifetime spectroscopy. *Journal of Applied Physics* 2007; **101**: 033710, 1–6.
6. Birkholz JE, Bothe K, Macdonald D, Schmidt J. Electronic properties of iron-boron pairs in crystalline silicon by temperature- and injection-level-dependent lifetime measurements. *Journal of Applied Physics* 2005; **97**: 103708, 1–6.
7. Roth T, Rudiger M, Diez S, Trupke T, Bardos RA, Glunz SW. Analysing defects by temperature and injection dependent lifetime measurements. *21st European PVSEC*, Dresden, 2006.
8. Rein S, Diez S, Glunz SW. Temperature and Injection Dependent Lifetime Spectroscopy (TIDLS): Advanced analysis. *19th European PVSEC*, Paris, 2004.
9. Rein S, Glunz SW. Electronic properties of interstitial iron and iron-boron pairs determined by means of advanced lifetime spectroscopy. *Journal of Applied Physics* 2005; **98**: 113711, 1–12.
10. Macdonald D, Cuevas A. Trapping of minority carriers in multicrystalline silicon. *Applied Physics Letters* 1999; **74**(12): 1710–1712.
11. Cousins PJ, Neuhaus DH, Cotter JE. Experimental verification of the effect of depletion-region modulation on photoconductance lifetime measurements. *Journal of Applied Physics* 2004; **95**(4): 1854–1858.
12. www.instec.com, 08 August 2007.
13. Reggiani S, Valdinoci M, Colalongo L, Rudan M, Baccarani G, Stricker AD, Illien F, Felber N, Fichtner W, Zullino L. Electron and hole mobility in silicon at large operatingtemperatures. I. Bulk mobility. *IEEE Transactions on Electron Devices* 2002; **49**(3): 490–499.
14. Arora ND, Hauser JR, Roulston, DJ. Electron and hole mobilities in silicon as a function of concentration and temperature. *IEEE Transactions on Electron Devices* 1982; **29**: 292–295.
15. Dorkel JM, Leturcq P. Carrier mobilities in silicon semi-empirically related to temperature, doping and injection level. *Solid-State Electrons* 1981; **24**(9): 821–825.
16. McIntosh KR, Guo JH, Abbott MD, Bardos RA. Nonlinear response of the WCT-100 photoconductance instrument at low conductance. *Progress in Photovoltaics*, 2008; **16**: 279–287.
17. Istratov AA, Hieslmair H, Weber ER. Iron and its complexes in silicon. *Applied Physics A* 1999; **69**: 13–44.
18. Graff K. *Metal Impurities in Silicon-Device Fabrication*. Springer: Berlin, 1999.
19. Kimerling LC, Benton JL. Electronically controlled reactions of interstitial iron in silicon. *Physica B & C* 1983; **116**: 297–300.
20. Macdonald D, Geerligs LJ, Azzizi A. Iron detection in crystalline silicon by carrier lifetime measurements for arbitrary injection and doping. *Journal of Applied Physics* 2004; **95**: 1021–1028.
21. Obermeier G, Huber D. Iron detection in polished and epitaxial silicon wafers using generation lifetime measurements. *Journal of Applied Physics* 1997; **81**: 7345–7349.

DOI: 10.1002/pip